Highly nonlinear transport phenomena in fullerene based diodes

G. J. Matt*, T. Fromherz†, H. Neugebauer* and N. S. Sariciftci*

*LIOS, Physical Chemistry, Johannes Kepler University Linz, Altenbergerstraße 69, A-4040 Linz, Austria
†Institute for Semiconductor and Solid State Physics, Johannes Kepler University Linz, Altenbergerstraße 69, A-4040 Linz, Austria

Abstract. Voltage–current measurements of fullerene based diodes in the temperature range between 295 – 15 K are presented. At temperatures below 95 K and at high current densities the diodes exhibit a voltage instability with a voltage hysteresis for opposite current sweep directions. This observation is interpreted with the formation of highly conductive current filaments in the fullerene film.

Keywords: Fullerenes, electronic transport, hopping transport, mobility edges
PACS: 71.20.Tx, 71.23.An, 71.23.Cq, 71.30.+h, 72.20.Ee, 73.61.Wp

INTRODUCTION

Fullerenes and derivatives of fullerenes exhibit a very special case of organic compounds which may possess semiconducting, metallic and even superconducting properties [1, 2, 3]. As in most organic compounds the mobility of the free charge carriers is rather low and is for spin cast fullerene films in the order of $10^{-3}\,\mathrm{cm^2/Vs}$ [4]. The hindered transport can be described with capturing and thermal remission of the charge carries in and out of localized states (traps) [6]. According to this model the effective measured mobility is expected to decrease with decreasing temperature. In contrast to these considerations we report the conversion of fullerene films into a highly conductive state at low temperatures and high current densities in fullerene based diodes.

EXPERIMENTAL

Fullerene based diodes were prepared as follows: Indium–tin–oxide (ITO) covered glass substrates were cleaned in three steps with toluene, acetone and methanol in an ultra-sonic bath. An approximately 70 nm thick film of poly(3,4–ethylenedioxythiophene/poly(styrene sulfonate) (PEDOT:PSS) (Bayer AG) as metallic hole conductor was spin-coated on the ITO layer under ambient conditions. A methanofullerene [6,6]–phenyl C_{61}–butyric acid methyl ester (PCBM) film was then spin–coated from chlorobenzene solution (3% wt.) on top of the PEDOT:PPS covered substrate, resulting in a PCBM film of ≈ 150 nm thickness. A top contact was evaporated on the PCBM film under dynamic vacuum ($p = 7 \cdot 10^{-6}$ mbar) through a shadow mask and consists of a stack of lithium–fluoride (LiF) (0.7 nm), Al (70 nm) and Au (100 nm).

CP786, *Electronic Properties of Novel Nanostructures*, edited by H. Kuzmany, J. Fink, M. Mehring, and S. Roth

Voltage–current ($V-I$) measurements via applying an certain current density and measuring the resulting voltage drop between the ITO and the LiF/Al/Au electrodes have been performed in the temperature range from room temperature to 15 K.

RESULTS AND DISCUSSION

From the device structure and the energy–level diagram given in Fig. 1, a built–in voltage V_{bi} of ≈ 1 V is estimated from the energy difference between the lowest unoccupied molecular orbital (LUMO) of PCBM at -4.2 eV [5] and the Fermi level of PEDOT:PSS at -5.2 eV [5]. The low energy of the highest occupied molecular level (HOMO) of PCBM (-6.1 eV) [5] results in a large energy barrier of 0.9 eV between the Fermi level in the PEDOT:PSS contact and the HOMO of PCBM. This energy barrier effectively suppresses hole injection from PEDOT:PSS into PCBM. Therefore, for biasing the diode in forward direction (i.e. biasing the PEDOT/ITO contact positive with respect to the LiF/Al/Au contact) only an electron current is injected from the LiF/Al/Au contact into the LUMO of PCBM and no hole current has to be considered for this device.

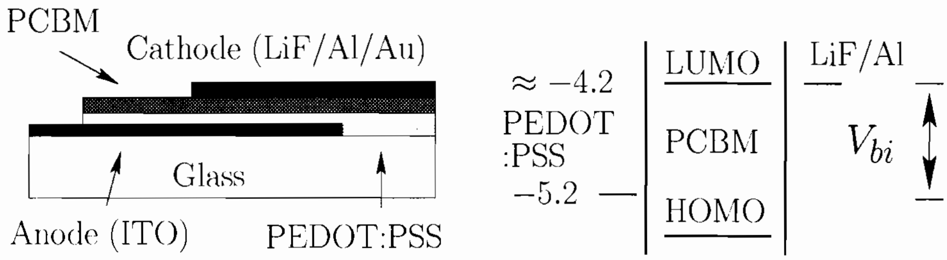

FIGURE 1. Geometric structure and energy-level diagram under flat band conditions for the PCBM based diode.

The current density for positive bias voltages features a power law dependency versus the effective applied bias voltage $V_{eff} = V - V_{bi}$ (see Fig. 2). Such an $I-V$ behavior is due to the formation of a space charge upon electron injection (space charge limited currents – SCLC) [6].

$$I \propto \theta \mu V_{eff}^2; \theta = n_f(E_f, 1/T)/n_t(E_f); E_f = f(V). \quad (1)$$

θ is the fraction of free to trapped charge–carrier concentrations n_f/n_t, μ is the microscopic mobility, T the absolute temperature and E_f is the average Fermi level in the PCBM film. At room temperature θ is a voltage independent value and the current density is proportional to the square of V_{eff} (see Fig. 2a). Lowering the temperature θ becomes voltage dependent and the current density is proportional to V_{eff} with a higher power than 2 (e.g $I \propto V^{3.3}$ at $T = 182$ K in Fig. 2). Below 95 K the regime in the $V-I$ dependence becomes temperature independent at high current densities (indicated by a $(*)$ in Fig. 2a and Fig. 3). Below 61 K the $V-I$ dependence features a voltage instability with a hysteresis for opposite current sweep directions (see Fig. 3). The hysteresis loops become more pronounced at lower temperatures and extend over larger area in the $V-I$ diagram (see inset in Fig. 3).

We interpret this observation as being due to a voltage dependent Fermi energy in PCBM and the formation of highly conducting current filaments between the diode contacts at low temperatures and high current densities [7]. The total number of trapped charges N_t, contributing to the space charge, is proportional to the applied bias voltage given by $N_t e = C \cdot V_{eff}$, where e is the elementary charge and C is directly related to the geometric capacitance. With applied bias voltage the trapped charges shift the Fermi level from E_{f0} (the Fermi–level when no bias voltage is applied) within the DOS of the traps (T–DOS) closer to E_c (the bottom edge of the conduction band; see Fig. 2b).

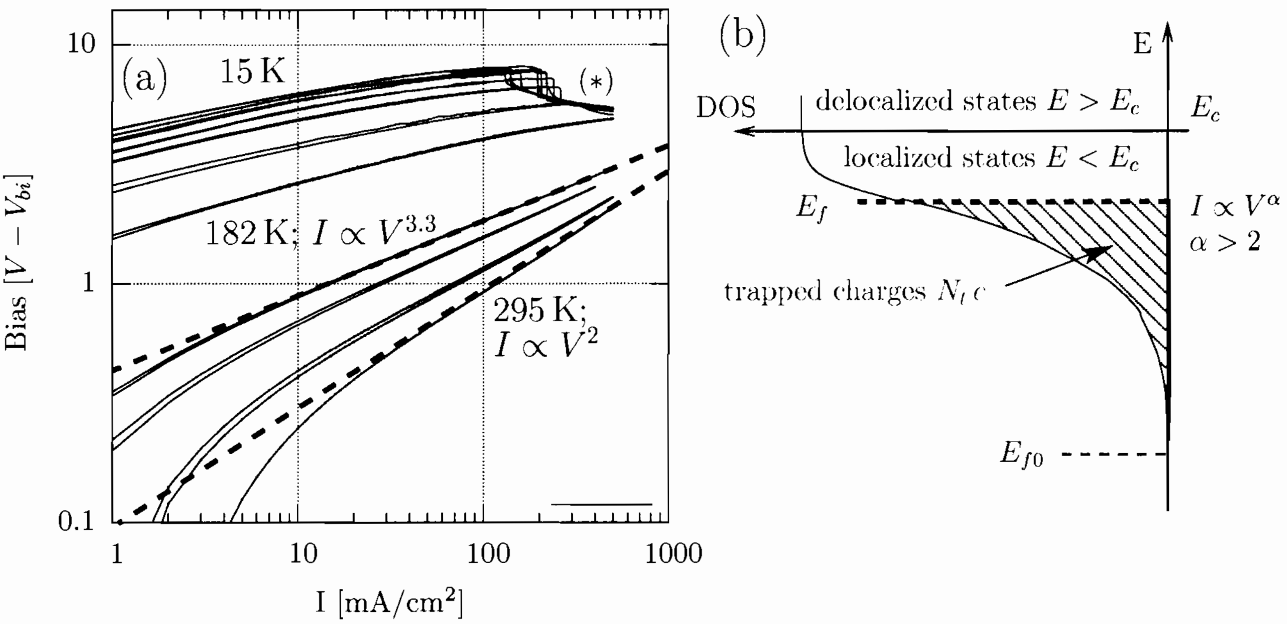

FIGURE 2. (a) Temperature dependent voltage–current density characteristics in double-logarithmic presentation. The dashed lines represent the $I - V$ power law dependency at two temperatures. The region with temperature independent $V - I$ characteristics is indicated by a $(*)$. (b) Density of states and the respective average Fermi level in the PCBM film.

As the energy of the Fermi level is increasing with increasing bias voltage, θ becomes voltage dependent and the current density is proportional to V_{eff} with a higher power than 2. At low temperatures and high current densities the Fermi level reaches E_c, the free charge carrier concentration is sharply increasing and the fullerene film forms a highly conductive state. This transition causes a voltage instability in the $V - I$ diagram. As the value of E_f is directly related to the T–DOS and the T–DOS is nonuniform along the PCBM film, E_f and the free charge–carrier concentration is also nonuniform. These inhomogeneities lead to the formation of highly conductive filaments in the fullerene film. The process is meta-stable featuring a hysteresis for opposite current sweep directions.

SUMMARY

We have observed an anomalous voltage–current density behavior of fullerene based diodes at low temperatures. The process is interpreted in terms of space–charge limited currents which alters the Fermi level close to the conduction band of the fullerene film. At low temperatures and high current densities the Fermi level reaches the conduction band and the fullerene film forms highly conductive filaments. This filamented state,

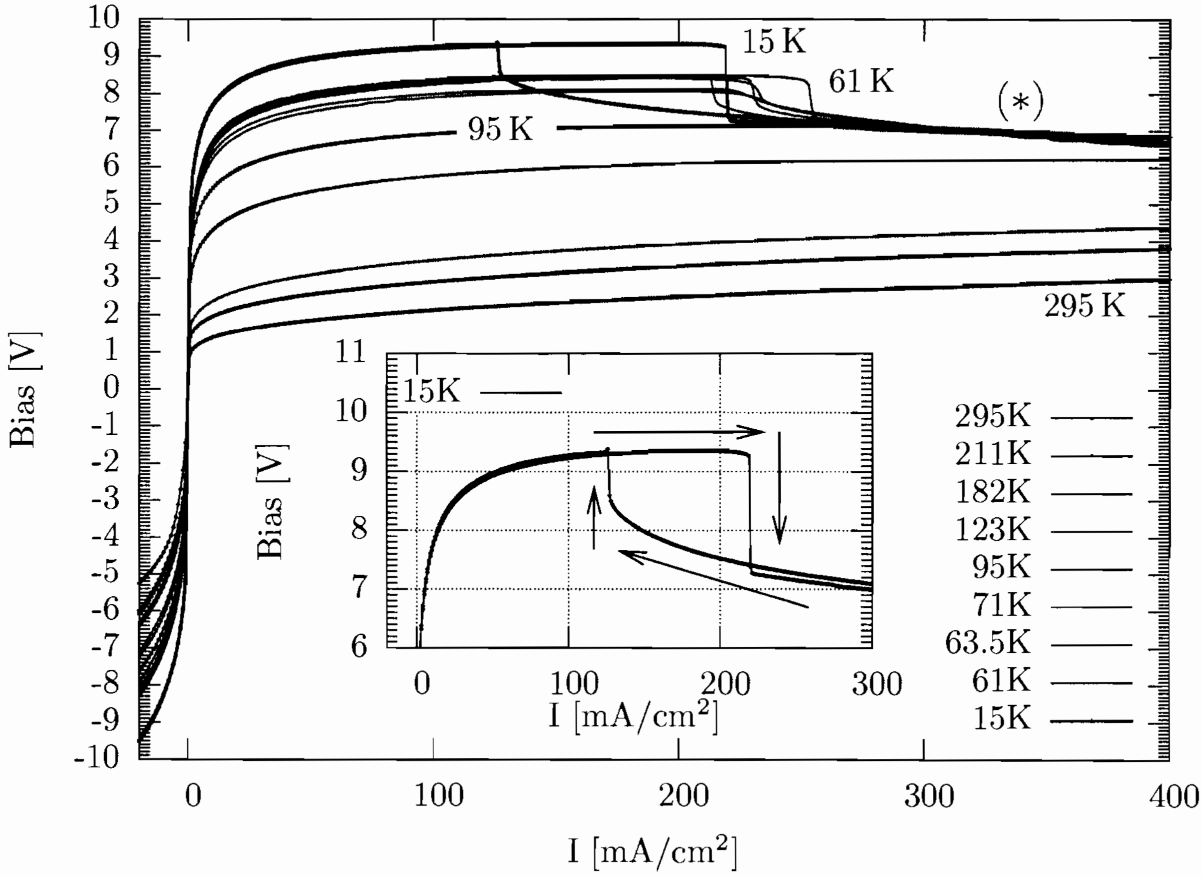

FIGURE 3. $V - I$ characteristics at various temperatures T from 295 to 15 K. The inset shows the hysteresis at 15 K in expanded scale. The region with temperature independent $V - I$ characteristics is indicated by a $(*)$.

which is metastable, shows a hysteresis for opposite current sweep directions and leads to a temperature independent $V - I$ behavior below 95 K and high current densities.

REFERENCES

1. M. S. Dresselhaus, G. Dresselhaus, and P. C. Eklund, *Science of fullerenes and carbon nanotubes.* Academic Press, Inc., (1995).
2. K. Tanigaki, I. Hirosawaand, T.W. Ebbesen, J. Mizuki, Y. Shimakawa, Y. Kubo, J. S. Tsai, and S. Kuroshima, *Nature* **356**, p. 419 (1992).
3. H. Sitter, A. Andreev, G. Matt, and N. S. Sariciftci, *Mol. Cryst. Liq. Cryst.* **385**. p. [171]/51 (2002).
4. G. J. Matt, T. Fromherz, and N. S. Sariciftci, *Appl. Phys. Lett.* **84**, 9, p. 1570 (2004).
5. C. Winder, D. Mühlbacher, H. Neugebauer, N. S. Sariciftci, C. Brabec, R. Janssen, and J. K. Hummelen, *Mol. Cryst. & Liq. Cryst.* **385**, p. 93 (2002).
6. A. Rose, *Phys. Rev.* **97**, p. 1538 (1955).
7. S. R. Ovshinsky, *Phys. Rev. Lett.* **21**, p. 1450 (1968).